Polar and midlatitude ozone

Daniel Cariolle[1,2], Sébastien Massart[1] and Hubert Teyssèdre[2]

[1] *Centre Européen de Recherche et Formation Avancée en Calcul Scientifique, 42 avenue Coriolis, 31057 Toulouse, FRANCE*
[2] *Meteo-France, Toulouse, FRANCE*
daniel.cariolle@cerfacs.fr

ABSTRACT

The objectives of this short article are to summarize our present understanding of the processes that control the stratospheric polar ozone content, and to show how those processes can control the distribution of the minor constituents of the polar stratosphere. Examples of modeling studies are reported to illustrate how chemical transport models forced by the ECMWF analyses can reproduce the ozone observations. The model simulations are further improved with the assimilation of satellite data, provided that the remaining inconsistencies between the measurements from the different O_3 measuring instruments are solved. It is concluded that in an operational perspective, the lack of availability of real time measurements is a major problem for improving the ozone analyses and forecasts.

1 Introduction

Since the discovery of the " hole of ozone " at the beginning of 1980s, our understanding of the mechanisms at the origin of the stratospheric ozone destruction improved. The measurement campaigns conducted in the Arctic and in the Antarctic, showed that the heterogeneous chemical processes at the surface of the particles of the polar clouds are at the origin of the preconditioning of the air masses and of the ozone destruction by chlorine and bromine radicals [12]. At the same time, the continuous monitoring of the atmospheric ozone content by satellites has demonstrated that the ozone destruction, initially confined inside the polar vortices, spreads at mid-latitudes under the influence of the propagation of large-scale planetary waves from the troposphere into the stratosphere. A continuous erosion of the vortices follows in winter and spring, which efficiently transports the polar air masses with low ozone contents towards the mid-latitudes. Figure 1 shows the annual mean tendency averaged over the last decade of the total ozone column. One can clearly see the footprint of the polar destruction that reaches its maximum in March in the northern hemisphere (NH) and in October in the southern hemisphere (SH), but also the signature of the ozone reduction at midlatitudes that persists in the SH over the summer months.

This tendency to the ozone destruction, recorded over a long time period, hides the large variability which is found from one year to another. In the SH this variability is linked to low-frequency phenomenon, notably the quasi-biennial oscillation which modulates the meridional circulation and the polar temperatures. In the NH, the destruction depends on the intensity of the planetary waves and their persistence throughout the winter. The ozone destruction in the NH winter is of the order of 10 to 30 % in the lower stratosphere at polar latitudes. These variations are in the range of those driven by the modulations of the meridional ozone transport from one year to another. It is thus important to set up a monitoring system of the atmospheric ozone content which can make quantitative evaluations of the tendencies due to ozone transport from those due to the chemical activity. In section 3 we describe how we can take into account, in a simplified manner, the chemical processes

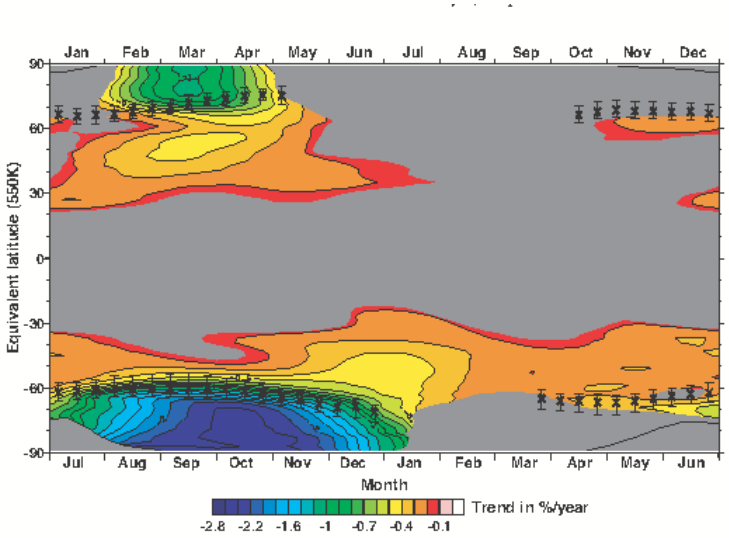

Figure 1: Ozone trend over the period 1978-2000 obtained from the analysis of TOMS and GOME data. Reprinted from WMO 2002 report [14]

controlling the ozone concentration in the general circulation models (GCMs), and how the assimilation of the satellite data can produce ozone fields showing a good consistency between transport and chemical processes.

2 Polar chemistry

The formation of the polar clouds is an essential element which determines the amplitude of the polar ozone destruction in the stratosphere. In the SH, the polar vortex forms in the stratosphere in winter from June to September. This vortex being relatively stable it remains centered over the pole, and the inside air masses cool gradually throughout the polar night. In spite of the very small humidities which prevail in the stratosphere, the temperature falls enough so that nitric acid trihydrate (NAT) and ternary solutions of HNO_3, H_2SO_4, and H_2O (STS) particles first form, followed by ice particles. In the lower stratosphere, it is considered that the NAT and STS particles form below about 195K. Below 189 K, particles grow and are mainly composed of ice.

Figure 2 shows the distribution of the cloud particles obtained by means of the MIPAS data from the ENVISAT satellite [7]. We see there clearly the formation of the particles of NAT and STS in border of the polar vortex, and those of ice inside the vortex where the temperatures are the lowest. The extension of the area covered by the PSCs increases from the end of May to mid-June, in a manner consistent with the progressive cooling of the air inside the vortex. In the NH, the polar vortex is less stable, the temperatures are higher, and the occurrence of the polar clouds decreases. As a consequence, the chemistry of the stratosphere will be less disturbed by the heterogeneous chemistry in the northern hemisphere than in the southern hemisphere.

The heterogeneous chemistry is effective at the surface of the PSCs particles and leads to the transformation of the nitrogenous radicals NO, NO_2 and N_2O_5 into nitric acid HNO_3. This last species remains trapped in the particles which can sediment to lower altitudes if the temperature remains cold enough. As a consequence, in the polar air which stayed for a long time in contact with clouds, nitrogen species have very low concentrations. This is for example illustrated by the trace species measurements obtained from the SMR instrument onboard

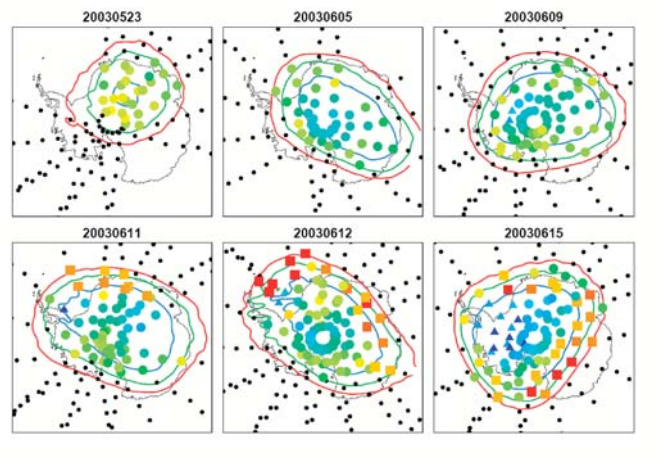

Figure 2: Distribution of PSC types at about 21 km derived from the MIPAS measurements over Antarctica during the 2003 summer. Red/orange are NAT particles, blue triangle are ice and blue-green circles are probably STS. Black dots are PSC-free observations. The contour lines are based on the ECMWF temperature analyses and enclose the ice existing region (blue), the STS region (green) and the NAT region(red). Reprinted from [7].

the ODIN satellite [10]. Figure 3 clearly shows that the NO_2 and HNO_3 concentrations are low in September inside the SH polar vortex.

At the same time, chlorine radicals are formed by the heterogeneous reactions of destruction of the reservoir species HCl and $ClONO_2$. The main reactions lead to the formation of Cl_2:

$$ClONO_2 + (HCl)_s \rightarrow Cl_2 + (HNO_3)_s \quad (1)$$
$$HOCl + (HCl)_s \rightarrow Cl_2 + (H_2O)_s \quad (2)$$

Cl_2 being rapidly photodissociated to form the Cl radical, and its oxide ClO by reaction between Cl and O_3.

As a consequence, in presence of polar clouds, the stratospheric air contains low concentrations of nitrogen oxides and high concentrations of chlorine radicals. This situation prevails almost every year at the end of the winter inside the SH polar vortex, and in a more variable way at high latitudes in the NH. In spring, with the return of the sunlight, the catalytic ozone destroying cycles can be very efficient. The main cycle involves the formation of the dimmer of the chlorine monoxide, Cl_2O_2:

$$\begin{aligned} ClO + ClO + M &\rightarrow Cl_2O_2 \\ Cl_2O_2 + h\nu &\rightarrow 2Cl + O_2 \\ 2(Cl + O_3 &\rightarrow ClO + O_2) \\ \hline 2O_3 &\rightarrow 3O_2 \end{aligned} \quad (3)$$

This cycle operates in the lower stratosphere if the temperatures remain low to prevent from the thermal decomposition of Cl_2O_2. If so, the ozone destruction rate due to the above cycle is a quadratic function of the ClO concentration, that itself is approximately equal to the total chlorine content since the concentrations of the chlorine reservoir species are low.

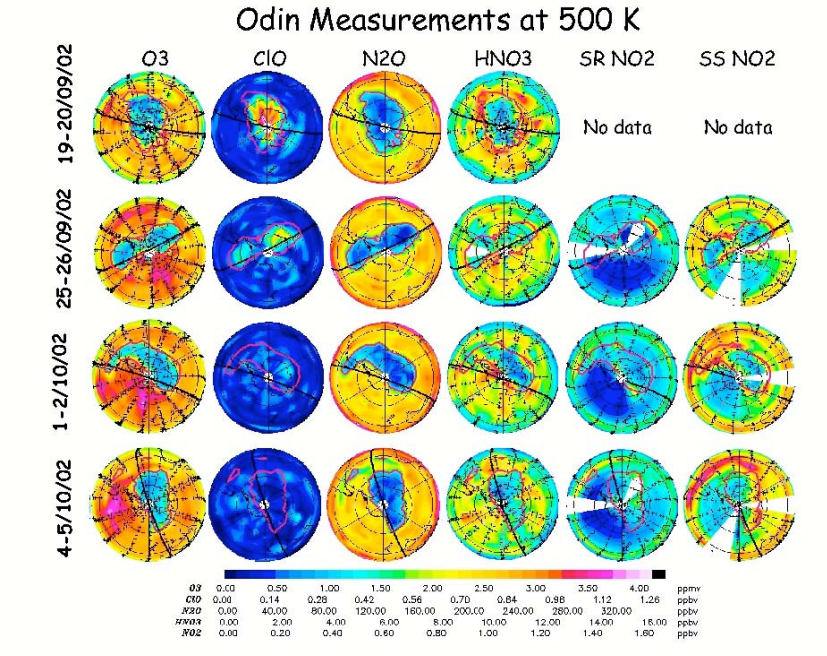

Figure 3: Distribution of minor stratospheric trace species observed in the SH spring using the ODIN satellite. Courtesy of Ph. Ricaud [10].

In addition to the above cycle, the following catalytic cycle that involves the bromine species must be taken into account:

$$\begin{aligned} BrO + ClO &\rightarrow Br + Cl + O_2 \\ &\rightarrow BrCl + O_2 \\ BrCl + h\nu &\rightarrow Br + Cl \\ Br + O_3 &\rightarrow BrO + O_2 \\ Cl + O_3 &\rightarrow ClO + O_2 \\ \hline 2O_3 &\rightarrow 3O_2 \end{aligned} \tag{4}$$

Given the concentration of the current bromine loading in the stratosphere, the bromine cycle typically accounts for about 30 % of the ozone destruction rate in the polar stratosphere. The above cycles can only be effective if the nitrogen oxide concentration is low, otherwise ClO will react with NO (reaction $ClO + NO \rightarrow Cl + NO_2$) or with NO_2 to form $ClONO_2$.

Figure 4 shows measurements of ClO and HNO_3 from the MLS instrument onboard the UARS satellite [11] during the period 1991-2000. In the Antarctic, the HNO_3 concentration decreases continuously from the end of May to July, and the ClO concentration has its peak value in September. This situation is fully consistent with our understanding of the chemical processes described above. In the Arctic, the inter-annual variability is much larger. In some winters the denitrification is high and the chlorine activation as well (1995-96; 1999-2000), and for other years, i.e. 1993-94, the HNO_3 concentration remains high and the ClO low. The different behavior from one year to another can be traced back to the history of the planetary waves amplitude. When

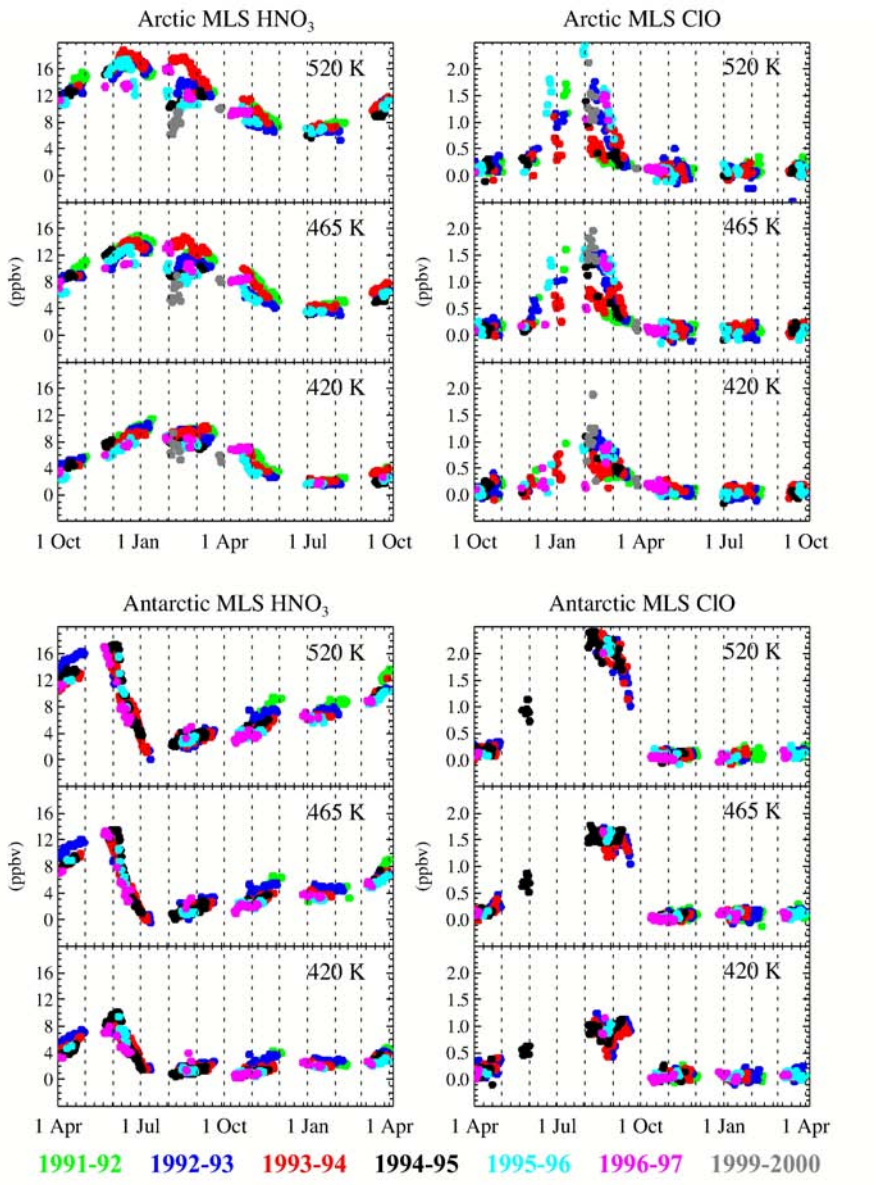

Figure 4: Time series of UARS MLS HNO_3 (left) and ClO (right) measurements at 420 K in the Arctic (top) and Antarctic (bottom). Reprinted from WMO 2002 report [14].

the wave amplitude is low during most of the winter, the polar vortex remains cold, centered over the pole and significant ozone destruction can occur in spring with the return of the sunlight. When the wave amplitude is large, the polar temperatures are higher, the air masses are not processed by heterogeneous reactions and the ozone destruction remains limited.

This variability in the planetary waves amplitude induces also large variations in the meridional ozone transport. In consequence, the evaluation of the net ozone destruction by chemistry is not easy. Recent evaluations, using chemical transport models (CTM), or based on analyses of the correlation between tracers and potential vorticity distributions, show that about 10 to 30 % of the arctic ozone is depleted in winter-spring in the lower stratosphere [14]. The next section discusses the prospects to improve those evaluations using chemical models coupled to assimilation of ozone data.

3 Modeling the polar and midlatitude ozone

In the previous section we showed that the observed minor species distributions agree qualitatively with our understanding of the key chemical processes at play in the lower polar stratosphere. In order to obtain more quantitative evaluations, one step further can be made with the comparison of CTM simulations with observations. Very often, CTMs use operational analyses of winds, temperature and humidity to solve the set of continuity equations for the minor species, i.e. [3]. The models are integrated for several years and, after a few months of spin up, the initial conditions do not influence much the solution, at least for the shorter lived species. For example, figure 5 shows the comparison between the measurements of O_3, ClO and N_2O from the SMR/ODIN with the corresponding outputs from the REPROBUS CTM forced with the ECMWF operational analyses [10]. The presented situation corresponds to the SH spring, with an increase of the ClO concentration and an ozone depletion inside the polar vortex. Low N_2O amounts are also find inside the vortex due to the subsidence that brings upper stratosphere air down to the lower stratosphere. The REPROBUS model catches quite well the large scale distributions of those minor species and their daily variability. This means that the representation of the transport and the chemical processes appears to be adequately accounted for.

In the context of forecasting the distribution of the minor species, in particular the ozone concentrations, the method of forcing a CTM with weather analyses and forecasts has several limitations. The first one is of course the demand on computing time. State of the art CTMs take account of at least 50 species coupled by about one hundred of reactions. This leads to the resolution of a large set of coupled continuity equations that often need specific solvers due to the stiffness brought by the large spectrum of the chemical species lifetimes. In practice, the time spent to integrate the CTM can encompass the one needed for the meteorological forecast, this becomes crippling with the current horizontal resolution of the forecasting systems.

The second limitation comes from the lack of constraints put on the chemical system, so that after several months of integrations drifts and biases can develop. This is first true for the long lived species, the distribution of which is going to be very sensitive to the dynamical balance of the forcing model. The possible biases in their amounts, i.e. N_2O, will impact the radical's content, i.e. NOx, and hence the other reactive species distributions, i.e. O_3. Biases and errors in the temperature distribution will also impact the chemical reaction rates. As described above, this is particularly important for the PSC related chemistry. To avoid those problems, additional constraints must be introduced in the modeling system. This can be done via the implementation of an assimilation system for the chemical species. Examples of assimilation of ozone vertical profiles are given below. But, considering the limited number of species measured in real-time, the information brought by the assimilation would be insufficient to constrain the whole chemical system.

Therefore, it makes sense to develop simplified chemical schemes in order to limit the number of continuity equations to be solved, and to restrict the approach to species that are measured at the global scale with spatial

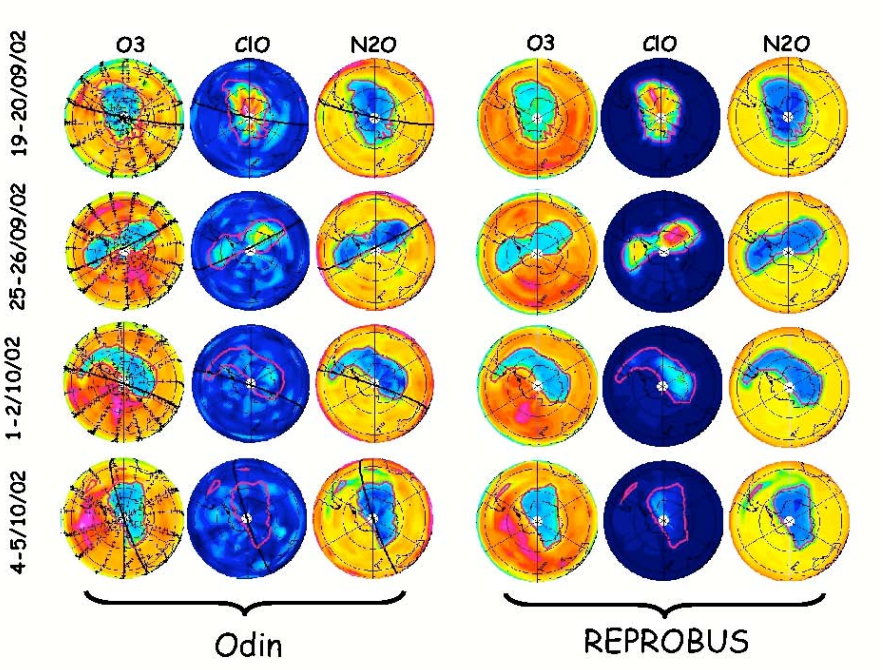

Figure 5: Distribution of O_3, ClO, and N_2O observed in the SH spring using the ODIN satellite, and modelled for the same dates by the REPROBUS chemical transport model. Courtesy of Ph. Ricaud [10].

and temporal resolutions coherent with those of the models. Such an approach is followed with the implementation within the ARPEGE/Climat and the ECMWF IFS models of the linear ozone parameterization of Cariolle and Déqué [1]. In that scheme the ozone continuity equation is expanded into Taylor series up to first order around the local value of the ozone mixing ratio, the temperature and the overhead ozone column:

$$\partial r_{O_3}/\partial t = A_1 + A_2(r_{O_3} - A_3) + A_4(T - A_5) + A_6(\Sigma - A_7) + A_8 r_{O_3} \tag{5}$$

where the A_i terms are monthly averages calculated using the 2D photochemical model MOBIDIC:

$A_1 = (P - L)$: Production and loss rate

$A_2 = \partial(P - L)/\partial r_{O_3}$

$A_3 = r_{O_3}$: ozone mixing ratio

$A_4 = \partial(P - L)/\partial T$

$A_5 = T$: temperature

$A_6 = \partial(P - L)/\partial \Sigma$

$A_7 = \Sigma$: ozone column

A_8: heterogeneous chemistry term,

whereas the other terms indicate the current 3D values of the ozone mixing ratio r_{O_3}, the temperature T, and the local overhead ozone column Σ, respectively.

The original scheme has been recently updated to account for PSC's ozone chemistry [2], and is currently in

operation in the ECMWF IFS model since February 2006. One advantage of this scheme is its good stability and lack of drift in long term simulations due to the relaxation towards the climatology of the 2D model. [2] discusses the CTM results when the linear scheme is used with forcing fields from the ECMWF operational analyses over the period 2000-2003. They found good agreement with Total Ozone Mapping Spectrometer (TOMS) data over that period, with a good representation by the model of the global distribution and the year-to-year variability of the total ozone column.

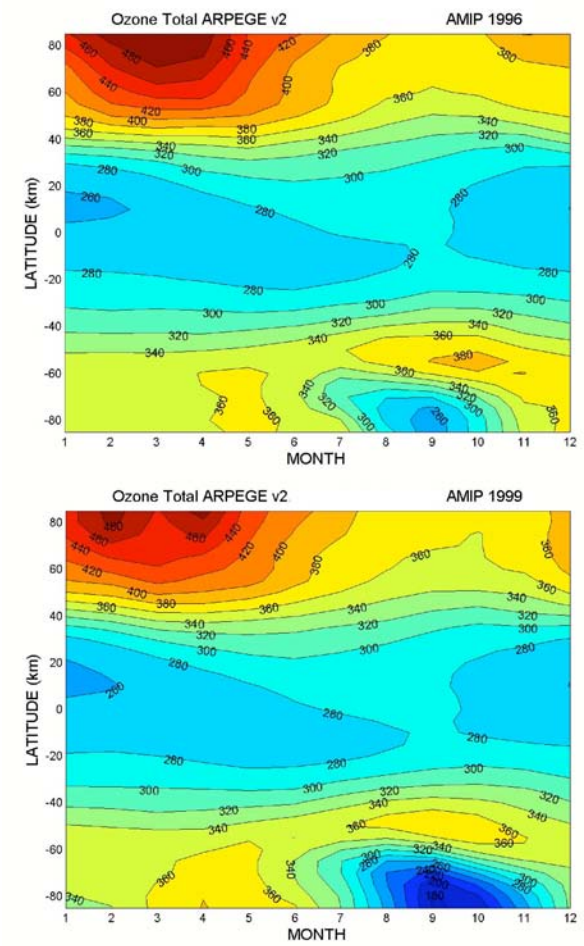

Figure 6: Time-latitude distributions of the total ozone column for two different years of a simulation of the ARPEGE/Climat model forced by observed sea surface temperatures over the period 1990-1999.

The linear scheme has also been introduced in the version 2 of the ARPEGE/Climat model [4] and a 10 year simulation has been performed with SST forcing from observations over the period 1990-1999. Figure 6 shows the total ozone column modeled over two different years. For both years the observed characteristics of the climatological ozone distribution are reproduced, with an equatorial minimum, spring maxima in the high northern latitudes, and a belt of high values around the polar minima in the SH in winter-spring. It is however interesting to see that during the first year the final warming occurs quite early at the end of September and is associated with rather high ozone content in the polar vortex. Whereas during the second year, the polar vortex is more stable, and the ozone hole formed in September persists until the beginning of November. In the NH, the second year shows two pulses in the large amplitude waves associated to meridional ozone transport,

and the first one presents a steady situation with larger ozone content over the pole. Those results show that, despite the simplicity of the linear scheme, free runs of the GCM give results as realistic as those of the CTM for reproducing a large part of the ozone column variability.

With the perspective of producing accurate ozone analyses and forecasts the forced CTM simulations are valuable, especially if the chemical system is introduced in a manner that prevent major biases and drifts. This appears to be the case with the linear model described above. However, it is anticipated that the model outputs would be further improved with the assimilation of ozone data.

At ECMWF the current ozone analysis is performed using SBUV vertical profiles and total ozone columns [5]. Other sources of data are now available, though not always processed fast enough to allow their use in the assimilation suite. This is the case for example with the Sub-Millimetre Radiometer (SMR) retrievals onboard the ODIN satellite [13] or the Michelson Interferometer for Passive Atmospheric Sounding (MIPAS) profiles produced by the D-PAC of ESA [9]. For the sake of illustrating how future operational models could use this data type, we briefly describe below some results of the assimilation of MIPAS and SMR profiles with the Météo-France Mocage CTM with implementation of the v2 linear ozone parameterization.

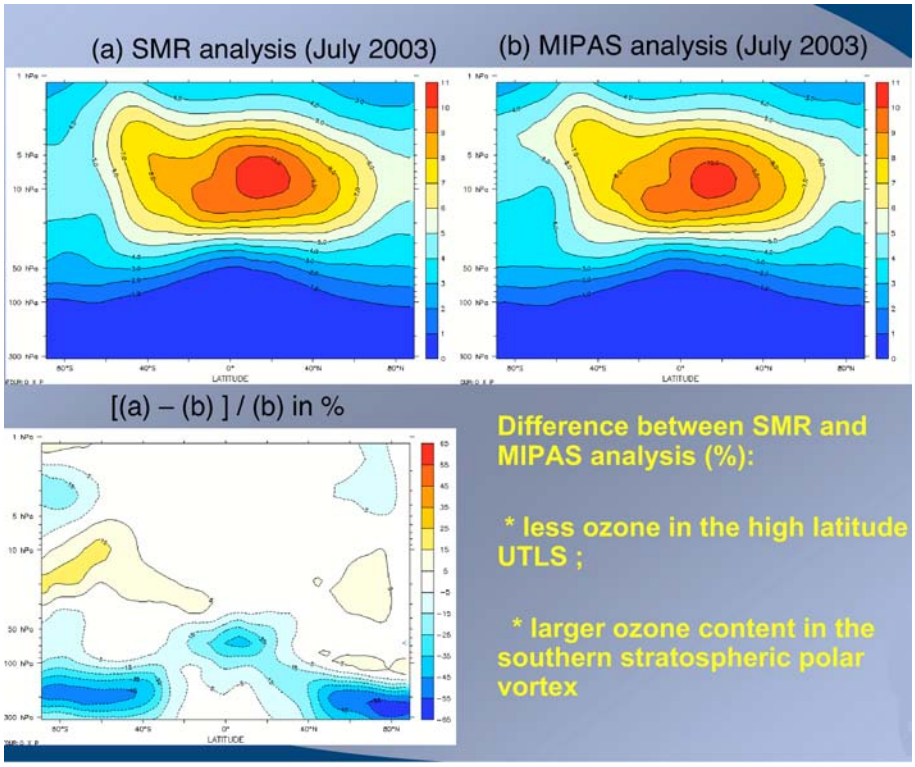

Figure 7: Averaged July 2003 zonal cross sections of the O_3 mixing ratio from the assimilation of SMR (upper left panel) and MIPAS (upper right panel) vertical profiles. Lower panel shows the zonal difference (in %) between the MIPAS and the SMR ozone analyses.

The method used is described in [8], and results from the assimilation of Global Ozone Monitoring Experiment ozone profiles with a 3D-First Guess at Appropriate Time (3D-Fgat) method are reported. The system has been further developed to assimilated MIPAS ozone profiles during the 2003 period (from July to the end of November) selected by the European project ASSET [6]. It gives ozone analyses of good quality compared to other assimilation systems and independent data.

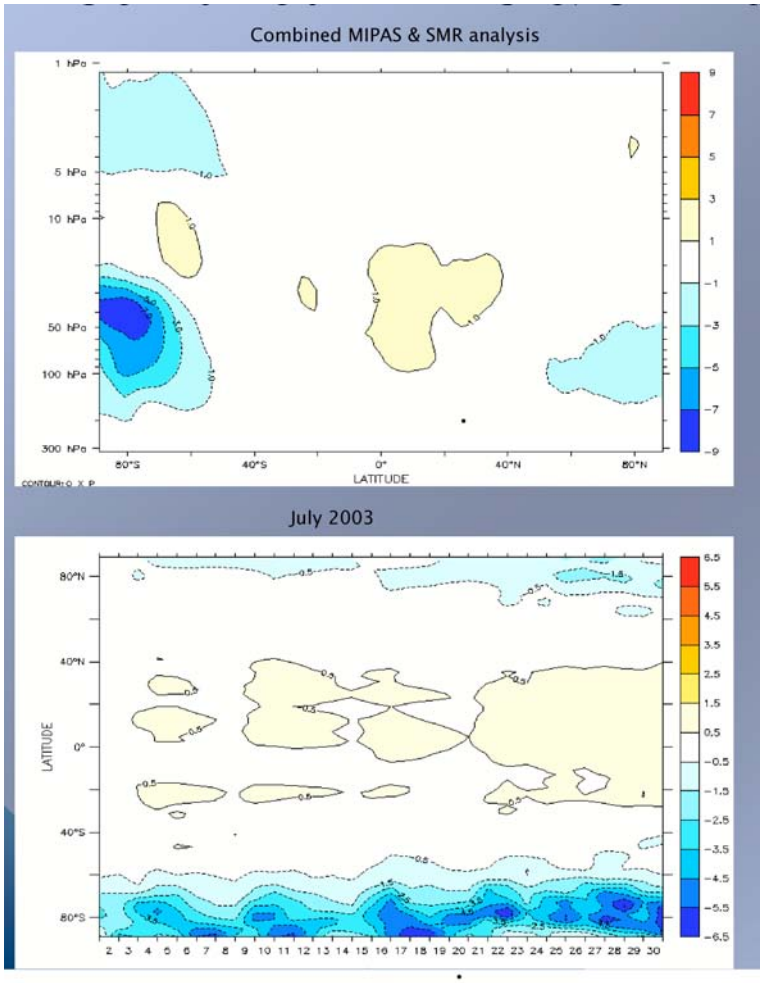

Figure 8: Averaged July 2003 zonal difference (in %) between the combined MIPAS-SMR and the MIPAS ozone analyses (upper panel), and the corresponding variations (in %) for the total ozone columns (lower panel).

Our assimilation system has been further extended, the upper boundary of the model now reaches the 0.1 hPa level, and the dynamical forcing comes from the operational IFS model. The assimilation can also cope with any instrument that gives vertical ozone profiles. Simulations have been performed using the MIPAS and the SMR data. Figure 7 shows the zonal mean cross sections of the stratospheric ozone for July 2003. At low and mid latitudes above 50 hPa the two assimilations give consistent results, with relative differences lower than 5%. At polar southern latitudes the assimilation using the SMR data gives ozone contents that are higher by 5 to 10 % compared to the MIPAS one above 40 hPa, but that are lower below that level.

In the upper troposphere lower stratosphere (UTLS), the MIPAS assimilation gives systematically higher values than the SMR one. Since there is no SMR data assimilated below 70 hPa, it means that the MIPAS data drive the model to a state where the ozone near the tropopause is much higher than the forced simulation without assimilation would produce. In the high northern latitude, the total ozone column produced by the MIPAS assimilation is higher than the TOMS data by about 5%. At polar latitudes in the SH there is no data from TOMS in July due to the polar night conditions and the comparison is not possible, but differences up to 8 % between TOMS and the MIPAS assimilation outputs are recorder later in the season. Thus, the high latitude ozone content produced by the MIPAS assimilation seems to be overestimated. Interestingly, the combined assimilation of both datasets (Figure 8) correct a large part of the bias in the lower stratosphere, despite that the number of MIPAS profiles (about 1200/day) is much larger than the SMR profiles (about 300 profiles per day). The correction is the largest at southern polar latitudes, with ozone reductions that can reach 7% locally and 4% for the total column.

4 Conclusion

In this paper we have discussed how chemical models can be validated against observations of the distribution of minor trace species. We conclude that current chemical transport models are able to take account of the main processes that drive the polar ozone destruction, but due to limitations in the forcing fields, biases and drifts can develop during the course of the integrations.

Simplified models, using for example linearised schemes for chemical rates, introduce further constraints in the system that can limit those biases and prevent from major drifts. Since they are easy to implement, and use very limited computer resources, they constitute a good choice for initial development of a forecasting system. Up to now, linear scheme are available for the computation of production and loss rates of ozone, but other species may be considered in the future.

The assimilation of minor trace species observations introduce further constraints in the system, and should lead to improved forecasts. The results however will be dependent on the space and time densities of the observations, and on the measurement errors. In the case of ozone, for which we have good quality measurements of the vertical distributions and the total columns, the combined analyses of the various datasets seem to be very promising. However, not all those observations are available in real time, and therefore they cannot be used for operational forecasting. They could however be used for re-analysis projects.

We have concentrated our discussions on the distribution of ozone in the stratosphere. In the troposphere the situation would be more complex because of the difficulty to model transport processes in the boundary layers, of the importance of liquid phase chemistry associated to clouds, and of the uncertainties in the ozone precursor emissions at ground level. In addition, observations of the distribution of minor trace species at the global scale, especially over the ocean, are available for a very limited number of species. This makes more difficult the development and the assessment of the quality of assimilation suites.

References

[1] Cariolle, D. and Déqué, M.: Southern hemisphere medium-scale waves and total ozone disturbances in a spectral general circulation model, J. Geophys. Res., 91, 10.825-10.846, 1986.

[2] Cariolle, D. and Teyssèdre, H.: A revised linear ozone photochemistry parameterization for use in transport and general circulation models: Multi-annual simulations, *Atmos. Chem. Phys.*, Submitted, acdp-0447, 2006.

[3] Chipperfield, M.: Multiannual simulations with a three-dimensional chemical transport model, J. Geophys. Res.,104, 1781-1805, 1999.

[4] Déqué, M., Dreveton, C., Braun, A. and Cariolle, D.: The ARPEGE/IFS atmosphere model: a contribution to the French community climate modelling, Climate Dynamics, 10, 249-266, 1994.

[5] Dethof, A. and Holm, E.: Ozone assimilation in the ERA-40 reanalysis project. Q. J. R. Meteorol. Soc., *131*, 2851-2872, 2004.

[6] Geer A. J., W. A. Lahoz, S. Bekki, N. Bormann, Q. Errera, H. J. Eskes, D. Fonteyn, D. R. Jackson, M.N. Juckes, S. Massart, V.-H. Peuch, S. Rharmili and A. Segers, The ASSET intercomparison of ozone analyses: method and first results, Atmos. Chem. Phys., submitted, 2006.

[7] Höpfner, M. , Larsen, N., Spang, R., Luo, B. P., Ma, J., Svendsen, S. H., Eckermann, S. D., Knudsen, B., Massoli, P., Cairo, F., Stiller, G., Clarmann, T. v. and Fischer, H: MIPAS detects Antarctic stratospheric belt of NAT PSCs caused by mountain waves. Atmos. Chem. and Phys., Vol. 6, pp 1221-1230, 20-4-2006.

[8] Massart S., Cariolle D., Peuch V.-H. Vers une meilleure représentation de la distribution et de la variabilité de l'ozone atmosphérique par l'assimilation des données satellitaires. C.R. Acad. Sci., 337-15, 13051310, 2005.

[9] Raspollini, P. , Belotti, C., Burgess, A., Carli, B., Carlotti, M., Ceccherini, S., Dinelli, B. M., Dudhia, A., Flaud, J. -M., Funke, B., Hpfner, M., Lopez-Puertas, M., Payne, V., Piccolo, C., Remedios, J. J., Ridolfi, M. and Spang, R.: MIPAS level 2 operational analysis Atmos. Chem. and Phys. Disc., Vol. 6, pp 6525-6585, 13-7-2006.

[10] Ricaud, P., Lefèvre, F., Berthet, G., Murtagh, D., Llewellyn, E.,J., Mégie, G., Kyrölä, E., Leppelmeier, G. W., Auviven, H., Boonne, C., Brohede, S., Degenstein, D.A., de la Noë, J., Dupuy, E., El Amraoui, L., Eriksson, P., Evans, W.F.J., Frisk, U., Gattinger, R.L., Girod, F., Haley, C.S., Hassinen, S., Hauchecorne, A., Jimenez, C., Kyrö, E., Lautié, N., Le Flochmoën, E., Lloyd, N.D., McConnell, J.C., McDade, I.C., Nordh, L., Olberg,M., Pazmino, A., Petelina, S.V., Sandqvist, A., Seppälä, A., Sioris, B.H., Solheim, B.H., Stegman, J., Strong, K., Taalas, P., Urban, J., von savigny, C., von Scheele, F., and Witt, G.: Polar vortex evolution during the 2002 Antarctic major warming as observed by the Odin satellite, J. Geophys. Res., 110, D05302, doi:10.1029/2004JD005018, 2005.

[11] Santee, M.L., G.L. Manney, N.J. Livesey, and J.W. Waters, UARS microwave Limb Sounder observations of denitrification and ozone loss in the 2000 Arctic late winter. Geophys. Res. Lett., 27, 3213-3216, 2000.

[12] Solomon, S., 1999: Stratospheric ozone depletion: A review of concepts and history, Rev. Geophys., 37, 275-316.

[13] Urban, J.; Lauti, N.; Le Flochmon, E.; Jimnez, C.; Eriksson, P.; d e La No, J.; Dupuy, E.; Ekstrm, M.; El Amraoui, L.; Frisk, U.; Murtagh, D.; Olberg, M.; Ricaud, P.: Odin/SMR limb observations of stratospheric trace gases: Level 2 processing of ClO, N2O, HNO3, and O3. J. Geophys. Res., Vol. 110, No. D14, D14307, 10.1029/2004JD005741,2005.

[14] WMO (World Meteorological Organization), Scientific Assessment of Ozone depletion: 2002, Global ozone Research and Monitoring Project - Report No. 47, 498 pp., Geneva, 2003.

Acknowledgments

The authors would like to thank H. Fisher and J. Urban from providing material on the results from the MIPAS and ODIN satellites that we have presented during the workshop.